JCB Report

Microtubule release from the centrosome in migrating cells

Miguel Abal,[1] Matthieu Piel,[1] Veronique Bouckson-Castaing,[1] Mette Mogensen,[2] Jean-Baptiste Sibarita,[1] and Michel Bornens[1]

[1]Institut Curie/UMR 144 du Centre National de la Recherche Scientifique, 75248 Paris, France
[2]School of Biological Sciences, University of East Anglia, Norwich, NR4 7TJ, UK

In migrating cells, force production relies essentially on a polarized actomyosin system, whereas the spatial regulation of actomyosin contraction and substrate contact turnover involves a complex cooperation between the microtubule (MT) and the actin filament networks (Goode, B.L., D.G. Drubin, and G. Barnes. 2000. *Curr. Opin. Cell Biol.*, 12: 63–71). Targeting and capture of MT plus ends at the cell periphery has been described, but whether or not the minus ends of these MTs are anchored at the centrosome is not known. Here, we show that release of short MTs from the centrosome is frequent in migrating cells and that their transport toward the cell periphery is blocked when dynein activity is impaired. We further show that MT release, but not MT nucleation or polymerization dynamics, is abolished by overexpression of the centrosomal MT-anchoring protein ninein. In addition, a dramatic inhibition of cell migration was observed; but, contrary to cells treated by drugs inhibiting MT dynamics, polarized membrane ruffling activity was not affected in ninein overexpressing cells. We thus propose that the balance between MT minus-end capture and release from the centrosome is critical for efficient cell migration.

Introduction

In animal cells, the centrosome acts as the main site of microtubule (MT)* nucleation; although, depending on the cell type, MTs can grow from other sites (Keating and Borisy, 1999; Schroer, 2001). MTs nucleated at the centrosome may either remain anchored or be released, like in neuronal or epithelial cells (Ahmad et al., 1999; Mogensen et al., 2000). In these cell types, the function of released MTs can be addressed as MT targeting to peripheral sites is correlated with cell differentiation. In migrating cells however, where released MTs have also been observed, their function remains unknown. A major riddle is the lack of tools to specifically analyze the role of MTs released from the centrosome. For example, the dynein–dynactin complex, which has been shown to be instrumental for MT anchoring at the centrosome (Quintyne et al., 1999), participates also in other mechanisms, including the interaction of MT plus ends with the cell cortex (Schroer, 2001). In addition, high concentration of MTs in the centrosomal area precludes a direct and detailed analysis of MT behavior in that region. In a previous study, we showed that the daughter centriole, which in steady-state conditions seems devoid of associated MTs, could actually nucleate MTs that were immediately released (Piel et al., 2000). In neurons, it was also demonstrated that most MTs were nucleated at the centrosome, although no MT could be observed in the centrosomal region, as they were released through the severing activity of the protein katanin (Ahmad et al., 1999). These two results lead to the prediction that MTs should be released while they are still very short, being then transported away from the centrosome before they substantially elongate. Thus, to study MT release from the centrosome, we used techniques enabling the observation of short MTs. As a tool to specifically perturb the balance between MT capture and release at the centrosome, we also used moderate overexpression of the protein ninein: this protein is specifically associated with MT minus ends in various cell lines and has been proposed to participate in MT anchoring at the mother centriole (Mogensen et al., 2000; Piel et al., 2000).

Results and discussion

A direct evualuation of the number and behavior of short MTs is actually almost impossible in steady-state conditions, as any tubulin staining gives a signal proportional to the

The online version of this article contains supplemental material.

Address correspondence to Dr. Michel Bornens, Institut Curie/UMR 144 CNRS, 26 rue d'Ulm, 75248 Paris Cedex 05, France. Tel.: 33-1-42-34-64-20. Fax: 33-1-42-34-64 21. E-mail: michel.bornens@curie.fr

M. Abal and M. Piel contributed equally to this paper.

*Abberviation used in this paper: MT, microtubule.

Key words: microtubule anchoring; microtubule dynamics; ninein; EB1-GFP; cell migration

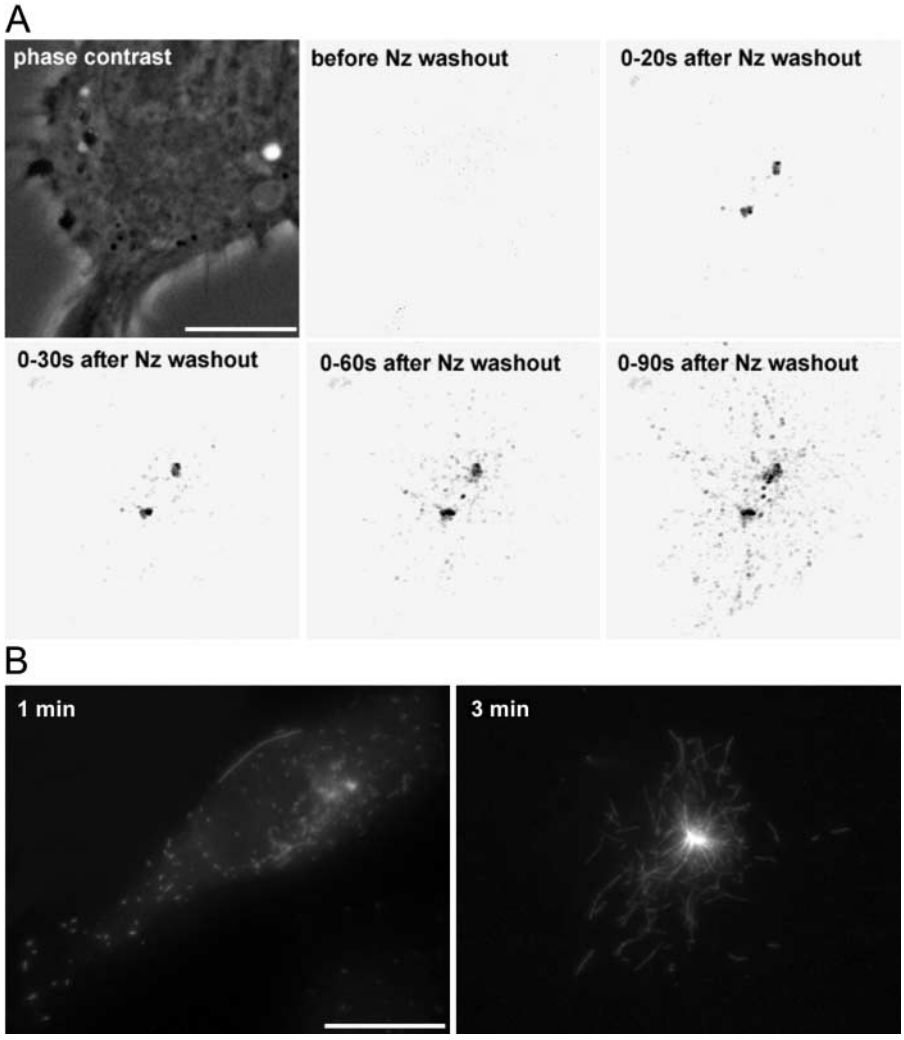

Figure 1. **Noncentrosomal MTs correspond to released MTs.** (A) MTs of L929 cells expressing EB1-GFP were fully depolymerized (2 h at 4°C, 10^{-6} M nocodazole). Cells were rewarmed in the presence of nocodazole and immediately recorded after nocodazole washout. Images were obtained by stacking consecutive images acquired every 2 s between indicated times. After deconvolution, images have been processed to extract fluorescence structures (EB1-GFP aggregates) from the background. Note that no EB1-GFP dot is visible in the cytoplasm until 20 s after nocodazole washout, but EB1-GFP accumulates around the two centrioles that are separated, as is almost always the case after microtubule depolymerization. After ~20–30 s, dots appear in the centrosomal region and spread throughout the cytoplasm during the next 60 s. Trajectories are mainly radial and emanate from the centrosome. The boundary of the cell can be estimated from the phase–contrast image (top, left). (B) Coverslips processed as in A were fixed 1 and 3 min immediately after recording and labeled with anti–α-tubulin antibodies. 3 min after regrowth, centrosomal and released MTs elongated. Video 1, demonstrating this process, is available at http://www.jcb.org/cgi/content/full/jcb.200207076/DC1. Bars, 10 μm.

length of individual MTs (in the speckle technique, the number of speckles is proportional to the length of the MT). Information on short MTs would thus be hard to extract with such an approach, which imposes a bias toward long MTs. We chose to record short-term regrowth experiments after total MT depolymerization. As tubulin background after MT depolymerization is too high to allow a direct observation of MTs regrowth with labeled tubulin, we used EB1-GFP as a marker of growing distal tips of MTs (Mimori-Kiyosue et al., 2000), followed by extraction/fixation of the recorded cells in order to visualize the MT network by immunostaining. In all cells recorded ($n = 10$), the great majority of EB1-GFP dots emanated from the centrosome and spread throughout the cytoplasm in <2 min (Fig. 1 A; and Video 1, available at http://www.jcb.org/cgi/content/full/jcb.200207076/DC1). EB1 dots began to leave the centrosome 20 s post nocodazole washout and were already 10 μm away at 1 min. On coverslips fixed after 1 min of recording, all cells contained short MTs associated with the centrosome, and numerous MTs (40 on average) spread throughout the cytoplasm (Fig. 1 B, left), but no MT of more than a few microns could be observed. Three minutes after regrowth, both centrosomal and noncentrosomal MTs of multiple sizes ≤10 μm were aboundant (Fig. 1 B, right), meaning that MT growth was not impaired by time-lapse recording. Moreover, similar images could be observed on coverslips fixed in the same conditions that had not been illuminated. We can thereby conclude that during the first minute of regrowth tens of short MTs are nucleated at the centrosome and then released.

The fact that these short released MTs can be found microns away from the centrosome in <1 min suggests that they are transported, probably by molecular motors. MT transport has already been demonstrated (Keating et al., 1997; Yvon and Wadsworth, 2000). It was also proposed that cortical dynein could pull on captured MT plus ends and thus transport them if their minus end is free (Smith et al., 2000). To ask whether short released MTs were transported by dynein, we overexpressed p150 CC1 (Quintyne et al., 1999). MT regrowth experiments showed that very few short MTs were found away from the centrosome after 1 min of regrowth in p150 CC1–expressing cells (Fig. 2 A, 1 min), whereas polymerization was not affected (Fig. 2 A, 3–5 min). We therefore conclude that in L929 cells, as reported for other cell types such as Ptk1 (Keating et al., 1997), MTs released from the centrosome are transported toward the cell periphery by MT minus end motors rather than by treadmilling only, which on the contrary was ob-

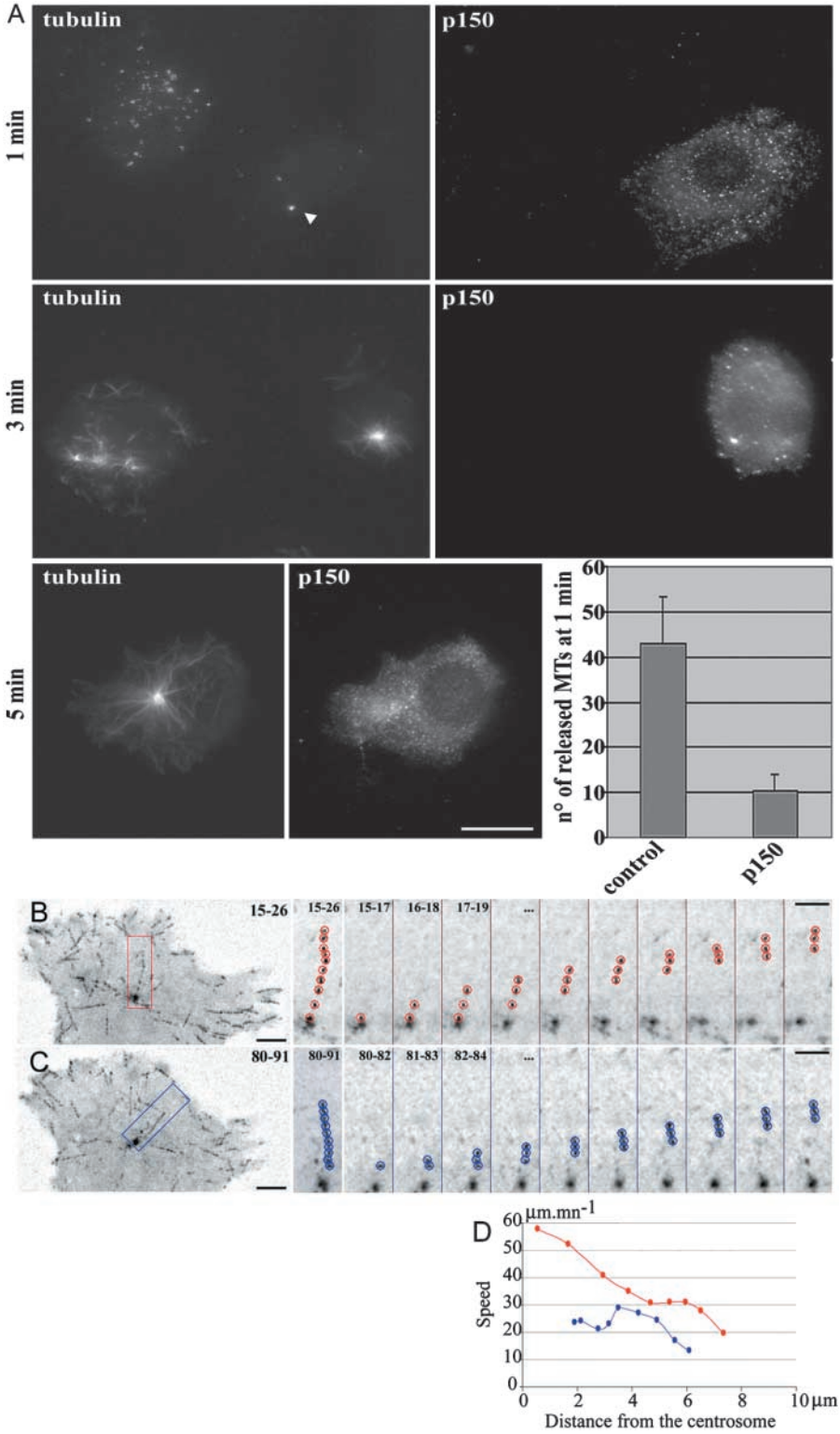

Figure 2. **Released short MTs are transported by dynein-dynactin complex.** (A) Inhibition of dynein–dynactin complex by p150 CC1-DsRed expression in L929 cells. Cells were treated as described in the legend to Fig. 1 and were fixed 1, 3, and 5 min after nocodazole washout. Cells were further stained with anti–α-tubulin antibodies, and p150 CC1-DsRed was visualized in the red channel. Note that almost no short MTs can be observed away from the centrosomal region (arrowhead) in the p150 CC1-DsRed–expressing cell. The number of noncentrosomal MTs has been estimated in control cells ($n = 12$) and in p150 CC1-DsRed–expressing cells ($n = 10$) (histogram); error bars indicate a 95% confidence interval calculated with Student's coefficient. (B–D) GFP signal in an EB1-GFP–expressing L929 cell. Images were obtained by stacking consecutive images acquired every second between times indicated in the upper right corner. Examples of EB1-GFP aggregates are shown either leaving the centrosome at a constant speed (C) or leaving the centrosome at a higher speed, and then slowing down (B). Sequential images on the right are a twofold blow up of the regions depicted on the left image. The speed of the particles is shown in D, as a function of their distance from the centrosome. Bars: (A and B) 10 µm; (D and E, left) 5 µm; (D and E, right) 3 µm.

served as the main feature in melanophores (Rodionov and Borisy, 1997). Furthermore, the fact that this transport could be observed in the absence of a MT network suggests that it is driven by motors anchored in cytoplasmic structures, like actin microfilaments (Garces et al., 1999), or intermediate filaments (Helfand et al., 2002). Strikingly, intermediate filaments are very abundant in the centrosomal region of L929 cells. Motors would be randomly dispersed; but if their concentration is high enough, it would be sufficient to explain the rather rectilinear movement of short MTs, as observed in in vitro motility assay.

We then reasoned that MTs released from the centrosome in steady-state conditions, when they are transported while elongating, should display an increased plus-end speed compared with those anchored at the centrosome. EB1-GFP recording could thus constitute a way to monitor release of

MTs. This technique allowed us to record, with a high temporal and three-dimensional spatial resolution, the speed of a considerable number of MT tips emanating either from the centrosome or from other places in the cell. We were indeed able to identify two subpopulations of MTs growing from the centrosome: the first characterized by a constant speed of EB1-GFP dots, compatible with polymerization (Fig. 2, C and D, blue track; 15–25 $\mu m/min^{-1}$, ~20% of MT tips emanating from the centrosome), and the second characterized by much faster movements away from the centrosome (Fig. 2, B and D, red track; 35–60 $\mu m/min^{-1}$, ~40% of MT tips emanating from the centrosome; the other 40% corresponding to speeds of 25–35 $\mu m/min^{-1}$, an intermediary speed, slightly faster than the usual reported polymerization speed). These MT tips usually slowed down to speeds compatible with polymerization as they approached the cell periphery (Fig. 2 D, red track). The speeds observed for the two populations suggest that they correspond respectively to polymerizing MTs anchored at the centrosome and to released MTs transported toward cell periphery by dynein, being finally tethered on other compartments or in the cortical cytoskeleton (Hoffmann et al., 2001). Recently, Komarova et al. (2002), using various approaches to estimate polymerization speed in the cell interior, reported values compatible with our slow moving population (17 ± 13.8 $\mu m/min^{-1}$). Fast-growing MTs anchored at the centrosome would have been detected by the techniques they used, ruling out the possibility that some anchored MTs could have an increased polymerization speed in the centrosomal area. On the other hand, these techniques could have missed short MTs moving at high speeds ($\leq$60 $\mu m/min^{-1}$), which require at least one image of plus-end labeling every second to be monitored. Alternatively, the cells used might have less released MTs than L929 cells, as very versatile MT behaviors were reported in various cell types. We thus conclude that, in steady-state conditions as in regrowth experiments, a subset of noncentrosomal MTs occurs through release from the centrosome and is subsequently transported toward the cell periphery.

We then wanted to specifically perturb that population of MTs by overexpressing the protein ninein. In L929, HeLa and human diploid primary fibroblasts (AFF11) cells, GFP-ninein protein specifically accumulated as a unique mass in the centrosomal area, similar to the endogenous localization at low expression levels (Fig. S1, available at http://www.jcb.org/cgi/content/full/jcb.200207076/DC1). No significant GFP signal was observed elsewhere in the cytoplasm. Ninein accumulation displayed a highly compact and ordered pattern, as revealed by EM. These features, which were also observed with the untagged protein, rule out the possibility that GFP-ninein accumulation at the centrosome corresponds to aggresomes of misfolded proteins. We also observed that GFP-ninein is functional and that, as expected, its accumulation increases MT anchoring capacity of the centrosome (Fig. S2, available at http://www.jcb.org/cgi/content/full/jcb.200207076/DC1).

To determine whether GFP-ninein overexpression could affect the production of short released MTs, we performed regrowth experiments as in Fig. 1. 1 min after nocodazole withdrawal, short MTs had been nucleated at the centrosome of both transfected and untransfected cells. But, when in control cells, numerous short MTs were observed throughout the cytoplasm, in overexpressing cells they were all confined to the centrosomal ninein accumulation (Fig. 3, A–C, quantification in G). Subsequently, three minutes after regrowth, both centrosomal and noncentrosomal MTs were observed in control cells, whereas in GFP-ninein–overexpressing cells, which contained a similar number of MTs, all MTs were associated with the centrosomal GFP-ninein accumulation (Fig. 3, D–F). This shows that accumulation of GFP-ninein at the centrosome does not perturb nucleation or elongation of MTs but suppresses released MTs.

We then analyzed the effect of ninein overexpression on the MT network in steady-state conditions. In cells exhibiting an accumulation of GFP-ninein at the centrosome, only the population of EB1-GFP dots with a constant lower speed could be observed (Fig. 3, H–M). In ninein overexpressing cells as well as in control cells, trajectories of EB1-GFP dots that did not seem to emanate from the centrosome were observed. This could, in most cases, be interpreted as rescues on MTs anchored at the centrosome as their inward prolonged trajectories reached the centrosomal area. Accordingly, these dots revealed speeds corresponding to the polymerization rate and were mainly observed in the lamellipodium area where most MT shrinkings and rescues were observed (see also Komarova et al., 2002), heading toward the cell periphery (Video 2, available at http://www.jcb.org/cgi/content/full/jcb.200207076/DC1). The proportion of noncentrosomal MTs occurring by breaking, spontaneous, or catalyzed nucleation at noncentrosomal sites could not really be estimated by the present technique. Nevertheless, we can state that only a minor population of EB1-GFP dots had either a nonradial trajectory or a radial movement toward the centrosome, corresponding to obvious nucleation at noncentrosomal sites or growth of a broken MT (a few percent of the total amount of EB1-GFP dots trajectories, compared with >20% for trajectories interpreted as MTs released from the centrosome in control cells). The cell periphery of ninein-overexpressing cells displayed a similar number of such EB1-GFP dot trajectories. That shows that, in steady-state conditions, ninein overexpression did not affect the dynamics of MTs near the cell periphery, or the production of free MTs by pathways other than centrosomal release. This suggests that MTs released from the centrosome are different from other noncentrosomal MTs: they might have a minus-end cap that ensures their stability, or bear particular cargoes because they were nucleated in the centrosome vicinity where many proteins are concentrated or activated.

We observed, by long-term phase–contrast video recording, that a moderate accumulation of GFP-ninein at the centrosome also correlated with a pronounced inhibition of cell migration, with a covered area less than half of that of the nontransfected cells (Fig. 4, A–B). Strikingly, inhibition of locomotion was due to a reduction in persistent migration in a given direction, whereas polarized membrane ruffling activity was not perturbed (Fig. 4, A and C; and Videos 3 and 4, available at http://www.jcb.org/cgi/content/full/jcb.200207076/DC1). This behavior was significantly different from that observed when cells were video recorded in

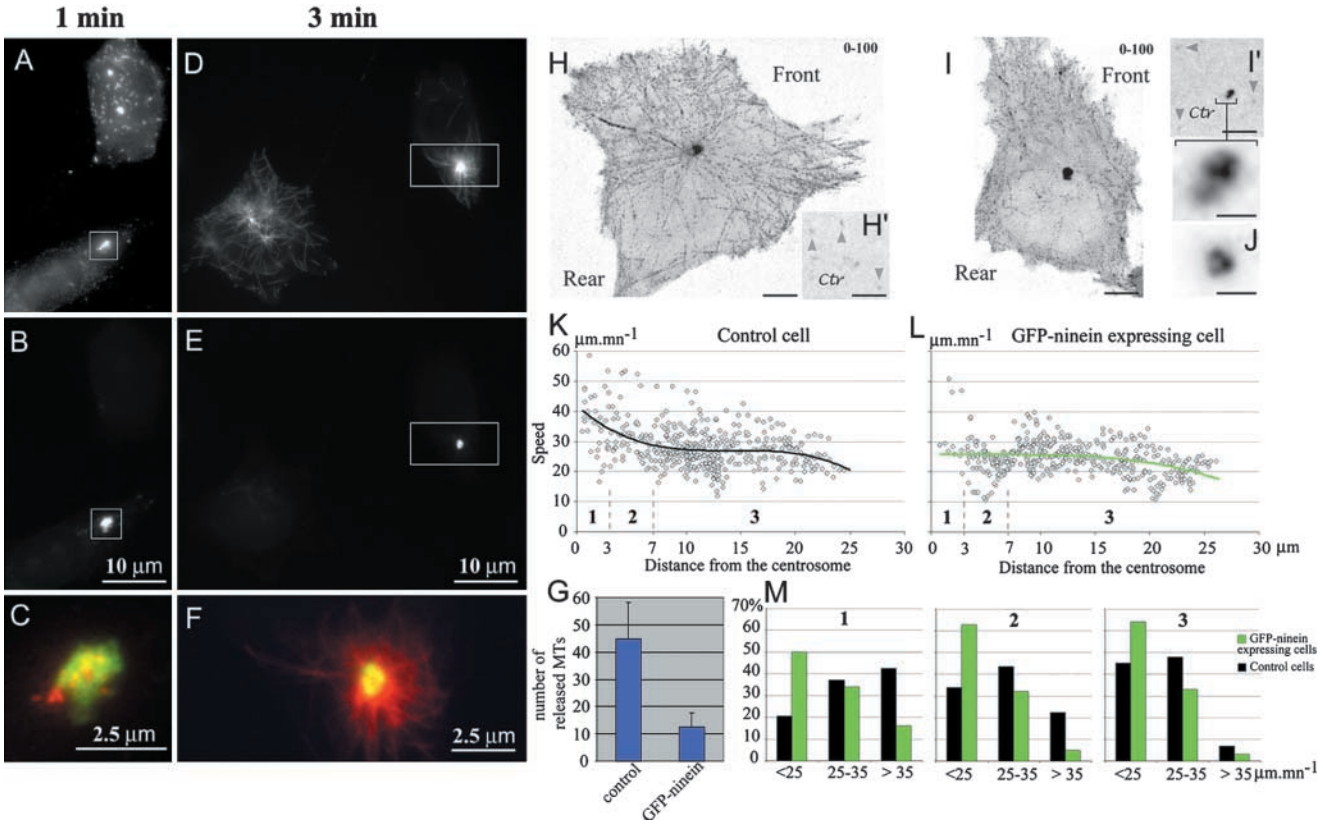

Figure 3. **GFP-ninein overexpression abolishes the release of MTs from the centrosome.** (A–G) GFP-ninein–transfected L929 cells were treated as described in the legend to to Fig. 1 and were fixed 1 (A–C) or 3 min (D–F) after drug removal. MTs were decorated with an anti–α-tubulin antibody (A and D), and GFP-ninein was visualized in the GFP channel (B and E). Note that noncentrosomal MTs are observed only in control cells and that nascent MTs are clustered within the ninein mass in GFP-ninein–overexpressing cells (merge in C and F of the outlined areas shown in A–E). The number of noncentrosomal MTs has been estimated in control cells (n = 12) and GFP-ninein–expressing cells (n = 10) (G). (H–M) EB1-GFP dynamics in control and in GFP-ninein–overexpressing cells. (H and H′) GFP signal in an EB1-GFP–expressing L929 cell; (I and I′) GFP signal in a L929 cell coexpressing EB1-GFP and GFP-ninein. Images were obtained as described in the legend to Fig. 2. Images in H′ and I′ are a detail of the centrosomal region of the cells shown in H and I at time 0, to show the actual staining of the centrosome without any stacking. The arrowheads indicate dots corresponding to EB1-GFP aggregates. Note, in H and I, the increased concentration of EB1-GFP dots in the lamellipodial regions at the front of both the control and the GFP-ninein–expressing cell. Only moderately overexpressing cells were considered for analysis: the sixfold blow-up of the centrosomal area of the GFP-ninein–overexpressing cell at the bottom of I′ is to compare with endogenous ninein in a control cell using an antibody, shown in J. (K and L) Speed of the EB1-GFP aggregates, tracked in the cells shown in H and I as a function of their distance from the centrosome. A polynomial fit has been added. Note the decrease of the mean speed in the first 10 μm around the centrosome in the control cell; whereas, in the GFP-ninein–expressing cell, the curve remains almost flat around 25 μm/min^{-1}. Three regions (1–3) have been distinguished around the centrosome, to make statistics over several cells. There are fewer points in region 1 or 2 than in region 3, because region 3 is where MT rescues are mainly observed, and because of a geometric effect (the surface increases with the square of the radius). (M) For both control condition and GFP-ninein overexpression, statistics were compiled from ∼2,000 EB1-GFP dots, corresponding to ∼200 MTs in 5 different cells. Note that the repartition of speeds in the GFP-ninein–overexpressing cells does not vary with the distance from the centrosome, whereas in control cells, an important population of transported MTs exist in the regions close to the centrosome (1 and 2). Video 2, corresponding to this figure, is available at http://www.jcb.org/cgi/content/full/jcb.200207076/DC1. Bars: (H, H′, I, and I′) 5 μm; (I′ blow-up and J) 1 μm.

the presence of low amounts of nocodazole (10^{-7} M), which do not depolymerize MTs but do inhibit their dynamic instability, or in the presence of paclitaxel (10^{-7} M). In both of these cases, a diminished ruffling activity was observed associated with a loss of cell polarity and motility (not shown), as also reported by others (Liao et al., 1995).

These data are thus compatible with a model in which dynamic MTs anchored at the centrosome regulate polarized regions of lamellipodial extensions (Wittmann and Waterman-Storer, 2001). By contrast, MTs released from the centrosome would be transported toward regions of lamellipodial extension and captured by the actin cytoskeleton. These noncentrosomal MTs are likely to be involved in the stabilization of the lamellipodia, which is necessary for efficient directed cell locomotion.

A direct effect of overexpressed GFP-ninein on lamellipodial dynamics is unlikely, as GFP-ninein was never observed at locations other than the centrosome in the cells used. Control overexpression of other centrosomal proteins in fusion with the GFP (centrin or γ-tubulin) did not affect cell migration. Our model is further supported by our observation that most released MTs are transported toward regions of lamellipodial extensions where they finally slow down, probably due to capture (Fig. 3, H and I; and Video 2). This fits with the description by others of detyrosinated MTs specifically enriched in the leading edge during directed loco-

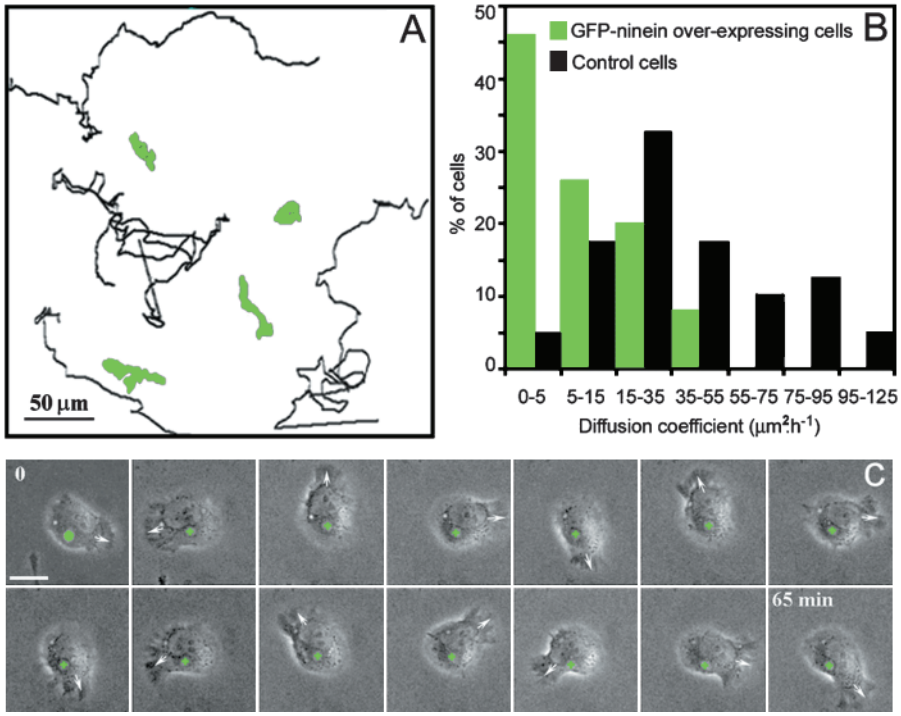

Figure 4. **Ninein accumulation at the centrosome inhibits cell migration.** (A) Representative examples of migration trajectories of GFP-ninein–expressing (green tracks) and –nonexpressing L929 cells (black tracks). (B) Histogram showing the distribution of the random migration values for control and GFP-ninein–overexpressing cells. Cell trajectories were characterized by the area covered by cell locomotion in a given time. Note the dramatic inhibition of random migration in GFP-ninein–overexpressing cells. (C) Time-lapse video recording of a GFP-ninein–transfected cell. The first picture is a superimposition of the fluorescence (green) and phase–contrast images; the centrosomal GFP-ninein accumulation is marked by a green cross in all other frames. Note that the centrosome remained almost completely static during the whole sequence, whereas the leading edge (arrow) rotated continuously. See also Video 3; Other cells could show a back and forth movement (Video 4). Videos are available at http://www.jcb.org/cgi/content/full/jcb.200207076/DC1. Bar: 10 μm.

motion (Gundersen, 2002). These MTs were also described as "curly," which could be indicative of a free minus end.

According to Kaverina et al. (1999), MTs could be targeted to focal adhesion plaques and modulate their turnover. We wondered whether the inhibition of locomotion observed in the absence of released MTs could be correlated to a reduced turnover of adhesion plaques or to an increase in stress fiber formation (Ballestrem et al., 2000). We found no difference in the size of the adhesion plaques, or in the organization of the actin cytoskeleton, between control and GFP-ninein–overexpressing cells. By contrast, cells treated with paclitaxel (10^{-7} M), presented larger adhesion plaques and more numerous stress fibers (Fig. S3, available at http://www.jcb.org/cgi/content/full/jcb.200207076/DC1). This indicates that the regulation of these structures, which are essential for membrane ruffling activity, depends on the dynamics of MTs rather than on their anchoring to the centrosome. How these released MTs affect cell locomotion still has to be worked out. It may involve the activity of small GTPases of the Rho family (Wittmann and Waterman-Storer, 2001; Fukata et al., 2002). The differential contribution of the daughter and the mother centriole to anchoring and release of MTs (Piel et al., 2000) may also, together with the plasticity of the intercentriolar linkage, be exploited in cell motility.

In conclusion, this work extends to migrating cells the importance of MTs released from the centrosome, already noticed in some differentiated cells. However, although in neurons and some epithelial cells, most of the MTs are released from the centrosome; this is not the case in migrating cells, where at least two distinct subsets of MTs coexist, each with specific functions in cell locomotion. Whether the balance between capture and release of MTs by the centrosome is modified in transformed metastatic cells with enhanced motility will deserve further study.

Materials and methods

Cell culture and transfection

AFF11 (primary foreskin human fibroblasts, obtained from Dr. Y. Barandon, École Normale Supérieure, Paris, France), HeLa, and L929 cells were grown in DME (GIBCO BRL), supplemented with 10% fetal calf serum (Eurobio). Exponential growing cells were transfected by electroporation as described (Piel et al., 2000).

Immunofluorescence

Cells transfected with GFP-ninein were processed as described (Piel et al., 2000). Images were taken using a Leica DMRXA microscope and 63×/1.32 or 100×/1.4–0.7 PL-APO objectives, a MicroMax charge-coupled device camera (Princeton Instruments), and IP-Lab or Metaview (Universal Imaging Corp.) software, and were processed using Adobe Photoshop.

Video microscopy

L929 cells were recorded from 12 h after transfection. Analysis of cell motility was accomplished by collecting phase–contrast (every 5 min) and fluorescence images (every hour) on a Leica DMIRBE microscope controlled by Metamorph software for ≥36 h. The microscope was equipped with an open chamber equilibrated in 5% CO_2 and maintained at 37°C, and images were taken with a 40×/0.70 PL Fluotar. To quantify cell motility, the area covered by a cell was determined using the root mean square of the excursion: $[<(X - <X>)^2> \times <(Y - <Y>)^2>]^{1/2}/2T$, where T is the total time of tracking, and X and Y the position coordinates of the cell.

Cells cotransfected with GFP-ninein and EB1-GFP to analyze MT dynamics were recorded by collecting fluorescent images every second. At each time point, the whole cell volume was scanned using a piezzo device mounted at the base of a 100×/1.4 PL-APO objective. MicroMax charge-coupled device cameras were used for acquisition, and Z stacks were deconvoluted and analyzed with Metamorph software.

Online supplemental material

In online supplemental Fig. S1, GFP-ninein specifically accumulates as a unique mass at the centrosome. In online supplemental Fig. S2, overexpressed GFP-ninein is functional and increases MT anchoring capacity in AFF11 cells. In online supplemental Fig. S3, inhibition of cell migration is not associated with obvious remodelling of adhesion plaques or actin cytoskeleton. Video 1 corresponds to Fig. 1 and shows EB1-GFP dynamics during MT regrowth. Video 2 corresponds to Fig. 3 and shows dynamics of growing MT plus ends. Videos 3 and 4 correspond to Fig. 4 and show inhibition of migration in ninein-GFP–transfected L929 cells. All

supplemental material is available http://www.jcb.org/cgi/content/full/jcb.200207076/DC1.

M.M. Mogensen thanks Birgit Lane and the Wellcome Trust for grants. The EB1-GFP and the p150 CC1-DsRed constructs were gifts from S. Tsukita and N.J. Quintyne, respectively.

M. Abal was supported by a grant from the Spanish MEC; M. Piel was supported by the Ligue pour la Recherche contre le Cancer; and this work was supported by a grant from the Human Frontier Science Program Organization to M. Bornens.

Submitted: 15 July 2002
Revised: 29 October 2002
Accepted: 31 October 2002

References

Ahmad, F.J., W. Yu, F.J. McNally, and P.W. Baas. 1999. An essential role for katanin in severing microtubules in the neuron. *J. Cell Biol.* 145:305–315.

Ballestrem, C., B. Wehrle-Haller, B. Hinz, and B.A. Imhof. 2000. Actin-dependent lamellipodia formation and microtubule-dependent tail retraction control-directed cell migration. *Mol. Biol. Cell.* 11:2999–3012.

Fukata, M., T. Watanabe, J. Noritake, M. Nakagawa, M. Yamaga, S. Kuroda, Y. Mutsuura, A. Iwamatsu, F. Perez, and K. Kaibuchi. 2002. Rac 1 and Cdc 42 capture microtubules through IQGAP1 and CLIP-170. *Cell.* 109:873–885.

Garces, J.A., I.B. Clark, D.I. Meyer, and R.B. Vallee. 1999. Interaction of the p62 subunit of dynactin with Arp1 and the cortical actin cytoskeleton. *Curr. Biol.* 9:1497–1500.

Goode, B.L., D.G. Drubin, and G. Barnes. 2000. Functional cooperation between the microtubule and actin cytoskeletons. *Curr. Opin. Cell Biol.* 12:63–71.

Gundersen, G.G. 2002. Evolutionary conservation of microtubule-capture mechanisms. *Nat. Rev. Mol. Cell Biol.* 3:296–304.

Helfand, B.T., A. Mikami, R.B. Vallee, and R.D. Goldman. 2002. A requirement for cytoplasmic dynein and dynactin in intermediate filament network assembly and organization. *J. Cell Biol.* 157:795–806.

Hoffmann, B., W. Zuo, A. Liu, and N.R. Morris. 2001. The LIS1-related protein NUDF of Aspergillus nidulans and its interaction partner NUDE bind directly to specific subunits of dynein and dynactin and to alpha- and gamma-tubulin. *J. Biol. Chem.* 276:38877–38884.

Kaverina, I., O. Krylyshkina, and J.V. Small. 1999. Microtubule targeting of substrate contacts promotes their relaxation and dissociation. *J. Cell Biol.* 146: 1033–1044.

Keating, T.J., and G.G. Borisy. 1999. Centrosomal and non-centrosomal microtubules. *Biol. Cell.* 91:321–329.

Keating, T.J., J.G. Peloquin, V.I. Rodionov, D. Momcilovic, and G.G. Borisy. 1997. Microtubule release from the centrosome. *Proc. Natl. Acad. Sci. USA.* 94:5078–5083.

Komarova, Y.A., I.A. Vorobjev, and G.G. Borisy. 2002. Life cycle of MTs: persistent growth in the cell interior, asymetric transition frequencies and effects of the cell boundary. *J. Cell Sci.* 115:3527–3539.

Liao, G., T. Nagasaki, and G.G. Gundersen. 1995. Low concentrations of nocodazole interfere with fibroblast locomotion without significantly affecting microtubule level: implications for the role of dynamic microtubules in cell locomotion. *J. Cell Sci.* 108:3473–3483.

Mimori-Kiyosue, Y., N. Shiina, and S. Tsukita. 2000. The dynamic behavior of the APC-binding protein EB1 on the distal ends of microtubules. *Curr. Biol.* 10:865–868.

Mogensen, M.M., A. Malik, M. Piel, V. Bouckson-Castaing, and M. Bornens. 2000. Microtubule minus-end anchorage at centrosomal and non-centrosomal sites: the role of ninein. *J. Cell Sci.* 113:3013–3023.

Rodionov, V.I., and G.G. Borisy. 1997. Microtubule treadmilling in vivo. *Science.* 275:215–218.

Piel, M., P. Meyer, A. Khodjakov, C.L. Rieder, and M. Bornens. 2000. The respective contributions of the mother and daughter centrioles to centrosome activity and behavior in vertebrate cells. *J. Cell Biol.* 149:317–330.

Quintyne, N.J., S.R. Gill, D.M. Eckley, D.A. Crego, D.A. Compton, and T.A. Schroer. 1999. Dynactin is required for microtubule anchoring at centrosomes. *J. Cell Biol.* 147:321–334.

Schroer, T.A. 2001. Microtubules don and doff their caps: dynamic attachments at plus and minus ends. *Curr. Opin. Cell Biol.* 13:92–96.

Smith, D.S., M. Niethammer, R. Ayala, Y. Zhou, M.J. Gambello, A. Wynshaw-Boris, and L.H. Tsai. 2000. Regulation of cytoplasmic dynein behaviour and microtubule organization by mammalian Lis1. *Nat. Cell Biol.* 2:767–775.

Wittmann, T., and C.M. Waterman-Storer. 2001. Cell motility: can Rho GTPases and microtubules point the way? *J. Cell Sci.* 114:3795–3803.

Yvon, A.M., and P. Wadsworth. 2000. Region-specific microtubule transport in motile cells. *J. Cell Biol.* 151:1003–1012.